

TRACKING SINGLE PROTEINS IN LIVE CELLS USING SINGLE-CHAIN ANTIBODY FRAGMENT-FLUORESCENT QUANTUM DOT AFFINITY PAIR

Gopal Iyer, Xavier Michalet, Yun-Pei Chang, *and* Shimon Weiss

Contents

1. Introduction	62
2. The Method: Targeting QDs via a Single-Chain Variable Fragment-Hapten Pair	64
3. Functionalization of QDs	66
3.1. Reagents for peptide coating	66
3.2. Peptide coating of QDs	66
3.3. Varying the stoichiometry of FL-pc-QDs	68
4. Quantification of the Number of FL Molecules per FL-pc-QD	69
5. Binding of FL-QDs to Anti-scFv Fusion Constructs	71
5.1. Quantification of the binding affinity of FL-QD to α -FL scFv	71
6. DNA Constructs for Single FL-QD Imaging in Live Cells	73
6.1. Labeling of live mammalian cells	74
7. Single-Molecule Imaging of Live Mammalian Cells	74
Acknowledgments	75
References	77

Abstract

Quantum dots (QDs) are extremely bright fluorescent imaging probes that are particularly useful for tracking individual molecules in living cells. Here, we show how a two-component system composed of a high-affinity single-chain fragment antibody and its cognate hapten (fluorescein) can be utilized for tracking individual proteins in various cell types. The single-chain fragment antibody against fluorescein is genetically appended to the protein of interest, while the hapten fluorescein is attached to the end of the peptide that is used to coat the QDs. We describe (i) the method used to functionalize QDs with

Department of Chemistry and Biochemistry, California NanoSystems Institute, University of California, Los Angeles, California, USA

fluorescein peptides; (ii) the method used to control the stoichiometry of the hapten on the surface of the QD; and (iii) the technical details necessary to observe single molecules in living cells.

1. INTRODUCTION

Fluorescence microscopy of live cells is a central tool in modern biological studies. The ability to adapt recombinant DNA methods for the fusion of fluorescent proteins (FPs) to target proteins in the cell, combined with the development of advanced light microscopy, has allowed researchers to explore trafficking of proteins, their turnover and localization (Lippincott-Schwartz and Patterson, 2003), cellular movement during embryogenesis (Kwon and Hadjantonakis, 2007), protein–protein interactions (Villalobos *et al.*, 2007), and cell lineage development in live cells (Wacker *et al.*, 2007) and whole organisms (Sakaue-Sawano *et al.*, 2008). Recent progress in use of fluorescence imaging in biology has gained from developments in optical instruments and imaging techniques (Betzig *et al.*, 2006; Michalet *et al.*, 2003; Westphal *et al.*, 2008), expansion of the FP repertoire (Chudakov *et al.*, 2005; Giepmans *et al.*, 2006), and introduction of quantum dots (QDs) (Bruchez *et al.*, 1998; Michalet *et al.*, 2005; Pons and Mattoussi, 2009). These advances, however, critically depend on the ease, versatility, and efficiency of fluorescently labeling macromolecules *in vitro* and *in vivo*.

Genetic encoding of proteins of interest with a FP is the most popular labeling method in cells (Tsien, 1998). Other modes of attachment of exogenous fluorophores to cellular proteins are based on (i) enzymatic strategies such as acyl carrier protein/phosphopantetheine transferase (George *et al.*, 2004); Q-tag/transglutaminase (Lin and Ting, 2006), biotin acceptor peptide/biotin ligase (Howarth *et al.*, 2005), prokaryotic hydrolase/Halo tag (Los *et al.*, 2008), formylglycine-generating enzyme/aldehyde tag (Carrico *et al.*, 2007), and Farnesyltransferase/CVIA peptide tag (Duckworth *et al.*, 2007); and (ii) noncovalent affinity labeling methods such as the tetracysteine/biarsenical system (Andresen *et al.*, 2004; Hoffmann *et al.*, 2005), dihydrofolate reductase (DHFR) (Miller *et al.*, 2004, 2005), the bis-arsenical/SplAsH (spirolactam Arsenical Hairpin binder) system (Bhunia and Miller, 2007), biotin/streptavidin (Weber *et al.*, 1989), and barnase/barstar (Wang *et al.*, 2004). QDs have emerged as a very promising class of fluorophores for multiple biological applications (Michalet *et al.*, 2005), including live cell imaging. Labeling cellular proteins with QDs depends on the way they are functionalized. Covalent and noncovalent attachment of proteins and small molecules to QDs can be achieved using standard conjugation chemistry (Michalet *et al.*, 2005).

One of the most interesting approaches has been to functionalize QDs with peptides. Peptide-coated QDs (pc-QDs) are advantageous (Iyer *et al.*, 2007; Pinaud *et al.*, 2004; Zhou and Ghosh, 2007) for several reasons: (i) The peptide coat is a natural cloak protecting the cell from the potentially toxic inorganic materials the QD is comprised of, (ii) exposed native functional groups such as $-\text{NH}_2$ and $-\text{COOH}$ can be manipulated by standard chemistries to react with the target of interest, and (iii) the stoichiometry of peptides with various reactive handles can be adjusted by varying the number and type of peptides displayed on the large surface of QDs. In particular, by tuning the functional peptide stoichiometry to one or few peptides per QD, it is possible to prevent or minimize the unwanted attachment of several target proteins to each QD.

A new frontier for fluorescence microscopy has recently emerged with the ability to observe single molecules in live cells, opening the way for a true molecular understanding of cellular processes (Hibino *et al.*, 2009; Joo *et al.*, 2008; Wennmalm and Simon, 2007). However, organic dyes and FPs are unfortunately prone to rapid photobleaching, limiting the time span of single-molecule observations. In addition, fluorescence saturation (asymptotic saturation of fluorescence at large excitation rates due to triplet blinking) and the finite fluorescence lifetime of fluorophores limit the temporal resolution of these single-molecule observations due to limited signal-to-noise ratio. Brighter and more stable fluorophores such as QDs have the potential to further our ability to explore fast as well as long-term single-molecule behaviors in live cells, by circumventing these two limitations. But since they are exogenous probes and cannot be genetically encoded, other means of targeting cellular proteins have to be developed. Furthermore, in order to harness QDs' tremendous potential for multicolor imaging, the development of several orthogonal targeting schemes will be necessary. The more conventional approach to address the QDs' targeting issue has been to directly attach primary (Watanabe and Higuchi, 2007) or secondary (Dahan *et al.*, 2003) antibodies to QDs. Although extremely versatile and simple (not requiring any modification of the target protein), this approach has several pitfalls. First, antibodies are large (as large as the QDs themselves), further increasing the size of the exogenous label, potentially interfering with the protein target's function. Second, antibodies are divalent, and since multiple antibodies could be bound to a single large QD, this raises the issue of multivalency of the probe and therefore of aggregation of the target. Third, antibody availability and specificity need to be addressed for each new protein of interest.

Direct attachment of the protein of interest to QDs by chemical cross-linking to an existing cysteine is a possible strategy, although it is easier to perform *in vitro* than *in vivo*. All other alternatives require modification of the protein sequence to add a chemical moiety that will allow binding to the functionalized QD. Several examples of such modifications already exist in

the literature. For instance, we recently showed how fusion of the chicken avidin sequence to a protein-moiety of interest allows its targeting by biotinylated pc-QDs at the single-molecule level (Pinaud *et al.*, 2009). Ting's group (Howarth and Ting, 2008) showed how enzymatic biotinylation of proteins allowed streptavidin-functionalized QDs to target these proteins. Dahan's group (Roullier *et al.*, 2009) designed, characterized and applied QD-trisNTA, which integrates tris-nitrilotriacetic acid, a small and high-affinity recognition unit for the ubiquitous polyhistidine protein tag. Direct visualization of protein-protein interactions at the single-molecule level was made possible for type-1 interferon subunits using a two-color QD tracking approach (Roullier *et al.*, 2009). Although quite powerful, these methods have their share of problems. In particular, avidin or streptavidin are tetramers with four binding sites for biotin, raising the possibility of multivalency. Also, these systems can only be used to target a single protein species at a time. Orthogonal binding schemes are still needed if several different proteins need to be targeted simultaneously. All of the approaches described earlier have merits; each can be used for a single protein target at a time, necessitating the mastery of different chemistries and strategies for multicolor labeling of several different species.

2. THE METHOD: TARGETING QDS VIA A SINGLE-CHAIN VARIABLE FRAGMENT-HAPTEN PAIR

To address these issues, we proposed a general strategy for targeting proteins with single QDs, based on the use of single-chain variable fragment (scFv) antibodies (Boder *et al.*, 2000) against small molecules (or haptens). The principle of our approach consists in fusing the scFv sequence to the cellular protein of interest and targeting it with QDs functionalized with the corresponding hapten. For a successful single-molecule tracking experiment, the QDs need to stay attached to the target protein for a long enough time, requiring a high-affinity interaction between the scFv and the hapten (in the range of a 10^{-12} to 10^{-15} M dissociation equilibrium constant).

Other hurdles in live cell experiments are nonspecific cellular labeling and a large molecular weight "penalty" of the fused affinity reagents (streptavidin: ~60 kDa and immunoglobulin IgG: 150 kDa). To circumvent these hurdles, we adapted a high-affinity scFv evolved against monovalent fluorescein (FL) ligand (Boder *et al.*, 2000). The anti-FITC scFv dubbed 4M5.3 (Boder *et al.*, 2000) is the highest known engineered affinity antibody to an antigen (FL) and has an affinity of 270 fM, a dissociation half-time of > 5 days and a low molecular weight of 30 kDa. The advantage of using anti-FITC scFv antibody for QD targeting (in lieu of GFP) is the possibility for long-term imaging (due to QDs' high brightness and

excellent photostability) together with such a high-affinity interaction. We therefore synthesized an N-terminal fluorescein isothiocyanate (FITC)-labeled peptide and used it to solubilize QDs. These coated QDs emit light in two colors (green from FITC and red from QD; [Iyer et al., 2008](#)). The ability to fuse the scFv's DNA sequence to genes expressed on the surface of a variety of cell types offers the possibility to simultaneously target several different-color QDs to different proteins by using (and further evolving) other high-affinity, orthogonal, scFv-hapten pairs. This approach is therefore well suited for monitoring and long-term tracking of individual proteins in cells and can be combined with multicolor labeling experiments with other color QDs and FPs. As an example, we generated hamster prion (PrP) DNA construct fused to this scFv and demonstrated that fusion of scFv to PrP does not impair its localization to the cell surface; we were also able to monitor its membrane diffusion by single-particle tracking of attached FITC-QDs ([Chang et al., 2008](#)), further showcasing the versatility of FITC-QDs as high-affinity binding partners.

A typical scFv has a molecular weight of 27 kDa which is comparable in size to a FP (e.g., eGFP: 30 kDa) and will therefore, in favorable cases, not interfere with the function of the protein to which it is fused. Genetic engineering of the protein fusion and its expression are in this respect similar to the standard approach used for the creation of FP-protein constructs, with similar advantages and inconveniences. However, used in combination with sparse labeling with hapten-functionalized QDs, it allows overcoming a major problem exhibited in FP-protein systems, which is the control of expression levels and thus, the amount of expressed-labeled proteins. By separating expression and labeling, our approach allows for external control of the degree of labeling of the target protein, by simply adjusting the concentration and incubation time of hapten-functionalized QDs.

Functionalization of the QDs with haptens is performed using our previously described peptide-coating technique ([Pinaud et al., 2004](#)). In this technique, a simple exchange reaction replaces the hydrophobic trioctyl-phosphine oxide (TOPO) molecules solubilizing QDs in organic solvent, by short (~ 20 amino acid (aa)) amphipathic peptides solubilizing QDs in aqueous buffers. By chemically grafting haptens to the peptide sequence (either before or after coating), the pc-QDs are equipped with the desired hapten. If needed, alternate methods for functionalizing QDs with a small hapten could be used instead of our peptide-coating approach.

The generality of this method comes from the availability of a growing number of scFvs against various haptens developed for various purposes and characterized by very small (tight) dissociation constants ([Brichta et al., 2005](#)). The availability of many such "affinity pairs" allows for orthogonal labeling of multiple targets with different-color QDs. Here, we illustrate this approach with the particular case of the 4M5.3 scFv (α -FL scFv) developed against FL by the Wittrup group. This affinity pair is characterized by a

dissociation constant of 270 fM in phosphate-buffered saline (PBS) and 48 fM in low salt buffer (Boder and Wittrup, 2000). We call the resulting QDs FL-pc-QDs, for FL-functionalized pc-QDs. As will become clear later, an advantage of using FL as hapten is the ability to quantify the presence and stoichiometry of the hapten on QDs. In the following, we fully characterize this system, demonstrate targeting of single FL-pc-QDs to scFv displayed on the surface of live yeast cells and, finally, show an example of long-term tracking of individual scFv-PrP fusion proteins in live neuronal cells. The fluorophore of choice needs to be a good single-molecule fluorophore, with good photostability, high quantum yield (which results in a better signal-to-noise ratio using less laser pumping power), large extinction coefficient, and low residency time in the triplet state (which produces interruptions of fluorescence emission).

3. FUNCTIONALIZATION OF QDS

Synthesis of QDs is reviewed elsewhere (Murray *et al.*, 1993; Peng *et al.*, 1997). In short, it is usually carried out at high temperatures from organometallic precursors in the presence of coordinating solvents. At the end of the reaction QDs are capped with a mixture of TOPO and alkyl amines, rendering them hydrophobic and not amenable for biological applications. Several methods exist to solubilize them in water, including lipid micelles, encapsulating TOPO with silica coating, or exchanging the hydrophobic coating with amphiphilic ligands. QDs can either be synthesized in house with the appropriate equipment, or purchased from various vendors such as Invitrogen Corporation, Evident Technologies, Ocean Nanotech, and others.

3.1. Reagents for peptide coating

Crude peptides with sequence FITC-GSESGGSESGFCCFCCCFCCF-CONH₂ (FL-peptide, FL-P) and KGSESGGSESGFCCFCCCFCCF-CONH₂ (K-peptide or K-P) were purchased from Anaspec (San Jose, CA). Polyethylene glycol reagents (PEG 330) were obtained from Pierce Biotechnology (Rockford, IL). All chemicals used for QD solubilization were purchased from Sigma-Aldrich (St. Louis, MO).

3.2. Peptide coating of QDs

1. TOPO-coated CdSe/ZnS QDs are synthesized as described by Dabbousi *et al.* (1997).

2. 20 μl of 1 μM TOPO-coated QDs are pelleted in a table top centrifuge at 10,000 rpm for 5 min in 10 volumes of methanol. The resulting pellet is resuspended in 450 μl of anhydrous pyridine and transferred to a 1.5 ml microcentrifuge tube labeled A. The pellet can be refluxed for few seconds at 60 °C on a heating top if the pellet is difficult to dissolve. Discard the QD solution if the pellet is particulate during the process of dissolution.
3. 4 mg of FL-P is weighed out and added to 50 μl of anhydrous DMSO in a 1.5 ml microcentrifuge tube labeled B. It is important to ensure that the peptide is dissolved completely. Place the tube in a water bath set at 60 °C with continuous monitoring if the pellet does not dissolve easily.
4. Pipette the pyridine containing QDs from tube A to tube B, immediately add 11.6 μl of tetramethyl ammonium hydroxide 25% (w/v) in methanol (Sigma), and vigorously mix the tube for few seconds.
5. Spin the tube at 12,000 rpm for 2–3 min in a high-speed microcentrifuge. Pour off the supernatant into a designated solvent waste container. Resuspend the pellet in 300 μl of anhydrous DMSO. Before adding DMSO, remove residual pyridine from the walls of the tube.
6. Prepare an Illustra NAP-25 gel filtration column (GE Healthcare) by equilibrating the column with distilled water 4–5 times per the manufacturer's instructions.
7. Load the column after the pellet has completely resuspended in DMSO. Do not vortex the pellet. Tube containing the QD pellet should be left standing at room temperature to dissolve slowly. The presence of aggregates during the process of dissolution indicates improper solubilization and should be discarded. Allow the DMSO containing QDs to settle into the column bed. Top the column with distilled water and monitor the band of QDs with a hand-held UV lamp.
8. Collect 1 ml of the QDs in a low-binding microcentrifuge tube. At this stage, QDs are solubilized with FL-P and can be used in a biological environment.
9. Measure the concentration of column-eluted FL-QDs at 493 and 607 nm with a scanning spectrophotometer using the extinction coefficients of FL 85,200 $\text{M}^{-1} \text{cm}^{-1}$ and QDs 353,762.8 $\text{M}^{-1} \text{cm}^{-1}$, respectively.
10. Dialyze the FL-QDs using a 300,000 MWCO cellulose ester or PVDF membrane (spectra/Por, Spectrum Labs, Rancho Dominguez, CA) against 4 l of PBS with frequent (3–4 times) change in the span of 6 h and overnight once. Dialysis should be carried out at room temperature protected from light.
11. Measure the concentration of column-eluted FL-QDs at 493 and 607 nm with a scanning spectrophotometer. Measuring before and after dialysis

will determine the final yield of the FL-QDs and will help in determining the scale of FL-QD synthesis required for all experiments.

12. To check colloidal properties, perform gel electrophoresis of the FL-QDs on a 1% agarose gel. Evaluate the presence of excess FL-P using a fluorescent gel scanner equipped with laser excitation at 488 nm or an imaging station equipped with a simple CCD camera with appropriate excitation and emission filters. If free FL-P are present at this stage, either attempt to repurify using a NAP-25 column or start over. A schematic representation of an FL-QD is shown in Fig. 3.1.

3.3. Varying the stoichiometry of FL-pc-QDs

Single-molecule experiments that involve affinity pairs should meet the following requirements: (a) The binding pair should have an affinity constant in the high picomolar to femtomolar range (see later), (b) affinity pairs should be orthogonal to each other (for multiplexing purposes) and otherwise inert (to minimize nonspecific labeling cross-reactivity), (c) should be small (nonperturbative to the cell), and (d) display single avidity and precise stoichiometry (to avoid cross-linking of targets inside the cell). We have

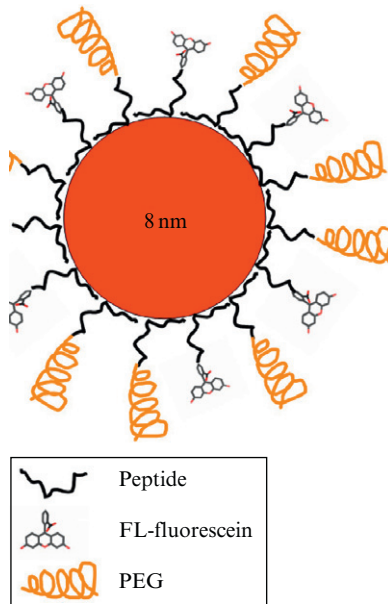


Figure 3.1 Schematic representation of QD functionalized with FL-P. Addition of polyethylene glycol to the pc-QDs minimizes nonspecific binding and sticking to surface during imaging.

been able to control the labeling density of the small hapten FL on the surface of QDs by varying the ratio of FL-P to NH_2 -peptide in the following way:

1. To obtain 100% FL-P coverage, follow the protocol as described earlier.
2. For 50% coverage, weigh out 2 mg each of FL-P and NH_2 -peptide, while for 10% coverage, weigh out 0.4 and 3.6 mg of FL-P and NH_2 -peptide, respectively, and proceed as described in [Section 3.2](#).
3. After dialysis into PBS, pH 7.4, unreacted amine groups can be blocked with small molecule PEG 330-NHS ester (Pierce, USA).
4. PEGylation can be carried out in PBS, pH 7.4, in 10–100-fold excess for 1 h at room temperature. The reaction is terminated by addition of 100 mM Glycine, pH 7.0, or any amine containing buffer. It is not necessary to remove the unreacted PEG as this does not interfere with downstream labeling applications.

4. QUANTIFICATION OF THE NUMBER OF FL MOLECULES PER FL-PC-QD

It is important to quantify the number of hapten molecules that cover the QD after conjugation. We have previously shown ([Iyer *et al.*, 2007](#)) that attaching a fluorescent label to the bioconjugated molecule can aid quantification of the resulting stoichiometry. A typical absorbance spectrum of FL-QDs is depicted in [Fig. 3.2](#).

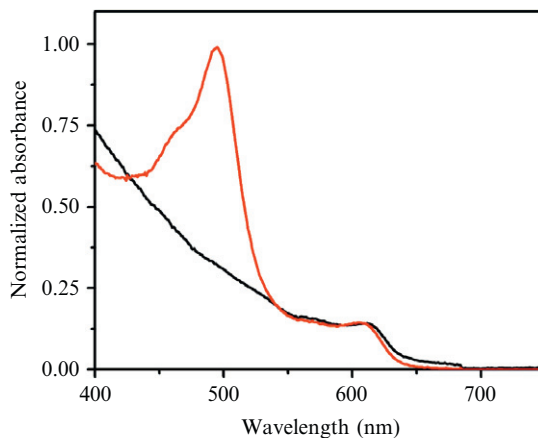


Figure 3.2 Normalized absorbance spectra of pc-QDs emitting at 620 nm. FL pc-QDs have absorption peaks at 493 and 610 nm, while pc-QDs have an absorption peak at 610 nm only.

A simple way to compute the number of FL-P coating each QD is by light absorption measurement. Absorption of light at a wavelength λ by a FL-pc-QD can have several causes: absorption by the QD if $\lambda < \lambda_{\text{QD}}$ (where λ_{QD} is the first exciton peak of the QD absorption), (ii) absorption by FL if $\lambda < \lambda_{\text{FL}}$ (where λ_{FL} is the upper limit of the absorption of FL), and (iii) absorption by the peptides themselves. The latter is negligible at visible wavelengths, and therefore it is easy to take measurements in two separate situations: one in which, first, only the QDs are absorbing ($\lambda_{\text{FL}} < \lambda < \lambda_{\text{QD}}$) and, second, where both FL and QDs are absorbing ($\lambda < \lambda_{\text{FL}} < \lambda_{\text{QD}}$). As we show next, these two measurements are sufficient to extract the number n of FL-P per QD using some simple assumptions and reference samples.

Let n be the unknown average number of FL-P per QD. The extinction coefficient of FL at 493 nm, $\varepsilon_{\text{FL}}(493)$, is provided by the manufacturer ($\varepsilon_{\text{FL}}(493) = 85,200 \text{ cm}^{-1} \text{ M}^{-1}$). The first exciton peak of the QD used in this experiment is 610 nm. If we measure the absorption of a FL-pc-QD at both 493 and 610 nm, we will obtain data corresponding to the two different situations described earlier. Assuming that the wavelength dependence of the QD and FL absorption spectra (i.e., the extinction coefficients) are not affected by the presence of the other species in close proximity, the total absorption at a wavelength λ will be:

$$A_{\text{FL-pc-QD}}\lambda = (\varepsilon_{\text{QD}}\lambda + n\varepsilon_{\text{FL}}\lambda)c_{\text{QD}}L, \quad (3.1)$$

where c_{QD} and L are the QD concentration and the excitation path length, respectively. The extinction coefficient of CdSe QDs (at their first exciton peak wavelength) has been experimentally measured by Peng and collaborators (Yu *et al.*, 2003) to depend on the first exciton peak wavelength according to:

$$\begin{aligned} \varepsilon_{\text{QD}} &= 5857D^{2.65} \\ D &= (1.6122 \times 10^{-9})\lambda^4 - (2.6575 \times 10^{-6})\lambda^3 \\ &\quad + (1.6242 \times 10^{-3})\lambda^2 - (0.4277\lambda + 41.57) \end{aligned} \quad (3.2)$$

where D is the diameter of the QD core in nm, and ε is expressed in $\text{M}^{-1} \text{ cm}^{-1}$.

From Eq. (3.2), we can calculate $\varepsilon_{\text{QD}}(610 \text{ nm})$, and by substituting it in Eq. (3.1) (written for $\lambda = 610 \text{ nm}$), obtain the QD concentration:

$$c_{\text{QD}} = \frac{A_{\text{FL-pc-QD}}(610)}{\varepsilon_{\text{QD}}(610)L}. \quad (3.3)$$

Writing Eq. (3.1) for $\lambda = 493$ nm, we obtain the following equation for n :

$$n = \frac{\left[\frac{A_{\text{FL-pc-QD}}(493)}{A_{\text{FL-pc-QD}}(610)} \varepsilon_{\text{QD}}(610) - \varepsilon_{\text{QD}}(493) \right]}{\varepsilon_{\text{FL}}(493)}. \quad (3.4)$$

The only unknown in this expression is $\varepsilon_{\text{QD}}(493 \text{ nm})$, which can be easily obtained from $\varepsilon_{\text{QD}}(610 \text{ nm})$ and the measurement of the QD-only absorption spectrum:

$$\varepsilon_{\text{QD}}(493) = \varepsilon_{\text{QD}}(610) \frac{A_{\text{QD}}(493)}{A_{\text{QD}}(610)}. \quad (3.5)$$

The number of FL-P per QD is thus given by the following equation:

$$n = \left[\frac{A_{\text{FL-pc-QD}}(493)}{A_{\text{FL-pc-QD}}(610)} - \frac{A_{\text{QD}}(493)}{A_{\text{QD}}(610)} \right] \frac{\varepsilon_{\text{QD}}(610)}{\varepsilon_{\text{FL}}(493)}. \quad (3.6)$$

The uncertainty in this number can be calculated by the standard rule of error propagation and can be kept below 1 if all parameters in Eq. (3.6) are affected by a relative error of a few percentages only.

5. BINDING OF FL-QDs TO ANTI-scFv FUSION CONSTRUCTS

After coating of the QDs with FL-P, the positive control yeast strain EBY 100 (*MATa ura3-52 trp1 leu2Δ1 his3Δ200 pep4::HIS3 prb1Δ1.6R can1 GAL* (pIU211:URA3) harboring plasmid pCT-4M5.3 (Boder *et al.*, 2000) can be used to confirm binding of FL-QDs to α -FL scFv (using both green and red fluorescence to detect FL and QDs, respectively). Growth and induction conditions of yeast cells have been described in Chao *et al.* (2006). Plasmids and strains can be requested from Dane Witttrup's lab, MIT, for testing individual preparation of FL-QDs.

5.1. Quantification of the binding affinity of FL-QD to α -FL scFv

Individual FL-QD preparations can be tested for binding affinity using yeast strain EBY 100 expressing α -FL scFv. This step is optional as our lab has determined that K_d values obtained with FL-QDs are sufficient to carry out single-molecule imaging experiments (Iyer *et al.*, 2008).

The method for measuring and determining the binding constant for FL-QDs is briefly described here. Although the α -FL scFv developed by the Wittrup group has a measured dissociation constant of 270 fM in PBS and 48 fM in low salt buffer (Boder *et al.*, 2000), this affinity concerns the free FL molecule. In our system, FL is cross-linked to a peptide, which is itself bound to a QD and is surrounded by other peptides and PEG molecules. This crowded environment could potentially reduce the affinity of α -FL scFv for the cross-linked FL species.

Briefly, incubate α -FL scFv expressing yeast cells with varying concentrations of FL-QDs and measure their total FL fluorescence. Plotting total FL as function of concentration should result in a sigmoidal curve, with $[\text{FL-QD}]_{1/2}$ being a characteristic concentration at which half of the change is observed (as expected for a simple single-step binding process). Growth, induction, labeling, and titration of FL-pc-QDs of 4M5.3 surface-displaying yeast are carried out as described previously (Chao *et al.*, 2006):

1. Incubate α -FL scFv-induced yeast cells with 1 pM to 600 nM FL-pc-QDs for 30 min at room temperature or 4 °C in low-binding microcentrifuge tubes on a rotator. The rotator should be incubated in the dark or the tubes be covered with aluminum foil.
2. Spin cells at 13,000 rpm for 30 s and wash pellet three times with 1 × PBS.
3. Transfer labeled yeast cells to FACS tubes.
4. Turn on BD FACSAria (Becton Dickinson, Franklin Lakes, NJ) flow cell sorter equipped with BD FACSDiVa software for at least 30 min. The cytometer has three lasers emitting at 488, 633, and 405 nm. The 488 nm laser excites FITC, whose emission is detected using a 530/30 filter. The 405 nm laser excites QDs, whose emission is detected using a 610/20 filter.
5. Obtain a forward versus side scatter profile for unlabeled yeast cells. If necessary, set compensation, although in our hands, a single control—cells stained for FITC indicated that no compensation was necessary. Compensation (PMT settings) may be required when using multiple fluorophores whose emission signals overlap.
6. Import FACS data in ASCII or txt format and analyze using software written in LabView (National Instruments, Austin, TX) to provide better control of the cell selection criteria (or gates).
7. Plot the (arithmetic) mean fluorescence signal of the gated cells in each channel (FL or QD). Make sure to reject cells with fluorescence signal < 0 (in either the FL or QD channel), which should correspond to cells with signal below background level when titrating with 10%, 50%, and 100% FL-QDs as described in Iyer *et al.* (2008).
8. Fit the percentage of cells retained for analysis with the same simple binding model (Chao *et al.*, 2006) used for the fluorescence signal itself. Obtain dissociation constants K_d for the FL and QD signal, respectively.

In summary, these measurements of the dissociation constant of the α -FL scFv/FL-QD pair using yeast as a model system can be optimized by the experimenter for further single-molecule imaging experiments in cells. We have observed that the increased dissociation constant measured (6.9 ± 5.1 nM) did not prevent single-molecule observation (as reported subsequently), showing that relatively large dissociation constants (in the nM) range are not an obstacle for this kind of application (Iyer *et al.*, 2008).

6. DNA CONSTRUCTS FOR SINGLE FL-QD IMAGING IN LIVE CELLS

A typical application for the FL-QD/4M5.3 affinity pair is to fuse 4M5.3 to the N- or C-terminus of a membrane or glycosphosphatidyl (GPI)-anchored protein. Fusions to cytoplasmic proteins have not been attempted especially since delivery of QDs into the cytoplasm is not straightforward and appropriate controls for folding of the 4M5.3 fusion protein has to be tested on a case-by-case basis. A typical DNA fusion construct for mammalian cells is illustrated in Fig. 3.3. To test if the FITC pc-QDs are suitable for single-particle tracking experiments in live mammalian cells, we designed the construct by fusing the anti-scFv 4M5.3 to a GPI-anchored protein so that the single-chain antibody is well exposed on the outer membrane. To construct anti-scFv 4M5.3-PrP fusion protein, the coding cDNA sequence of anti-scFv 4M5.3 was inserted to the immediate distal end of the signal peptide cleavage site (aa-23) of full length mouse PrP protein-bearing epitope 3F4 (Iyer *et al.*, 2008). The resulting construct is still anchored via the GPI anchor to the outer leaflet of the plasma membrane. The chimeric scFv-PrP construct is then cloned into mammalian expression vector pCDNA3 (Invitrogen) and transfected into mouse neuroblastoma cell line Neuro-2a (N2a, ATCC) using lipofectamine 2000 reagent (Invitrogen) following the manufacturer's protocol. Single stable clones are selected, isolated, and maintained by growth medium supplemented with 0.8 mg ml^{-1} G418 (Invitrogen).

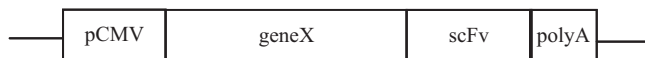


Figure 3.3 Schematic map of a mammalian DNA construct composed of gene X fused to single-chain fragment antibody anti-scFv 4M5.3 at the C-terminus. Similar fusions can be engineered to the N-terminus and also to GPI anchored protein. Reprinted with permission from Gopal Iyer *et al.* High affinity scFv- Hapten Pair as a Tool for Quantum Dot Labelling and Tracking of Single Proteins in Live Cells, Nano letters, 8 (12). Copyright 2008, American Chemical Society.

6.1. Labeling of live mammalian cells

This procedure can be adapted for most mammalian cell lines. Here, we describe the procedure for labeling mouse neuroblastoma cell line Neuro-2a (N2a from ATCC):

1. 35 mm culture dishes with No 1.0 or 1.5 glass bottom (Mattek Corp., MA) are coated with 0.1% poly-L-lysine for several hours, and then washed with PBS before cell plating.
2. Two days before microscopy experiments, N2a cells are plated at a density of 2×10^5 cells on the coated glass-bottom culture dish and maintained in DMEM supplemented with 10% (v/v) fetal bovine serum and $1 \times$ pen/strep (penicillin and streptomycin—100 \times stock). The cells are allowed to grow for 48 h at 37 °C with 5% CO₂.
3. Wash the cells once with Hank's buffer salt solution (HBSS, Invitrogen) to remove residual medium.
4. Block cells with 1% (w/v) bovine serum albumin (BSA) in HBSS for 1 h at 37 °C.
5. For ensemble labeling, incubate 1–10 nM FL-QDs with 1% (w/v) BSA in HBSS for 10 min at room temperature. For single-molecule imaging, use 2–10 pM FL-QDs under identical conditions.
6. Wash 4–5 times with HBSS buffer and if necessary, image cells using an epifluorescence microscope to optimize the wash conditions.
7. Uniform membrane staining should be visible in the green and red channels.

7. SINGLE-MOLECULE IMAGING OF LIVE MAMMALIAN CELLS

Single-molecule imaging experiments are carried out using total internal reflectance (TIRF) excitation (IX71, Olympus) and a high numerical aperture (NA) oil immersion objective (Olympus Planapo 60X, NA 1.45). The detection path is home-built and permits dual-color imaging, as described in [Pinaud *et al.* \(2009\)](#). Images are acquired by a back-illuminated EMCCD camera (Cascade 512B, Photometrics) controlled by the WinView software (Photometrics). Since a custom magnification is used, the size of the camera pixel in the object plane is calibrated using a reticle with 10 μ m pitch ruling. In our experiments, the pixel size was 95 nm per pixel. The lower limit on time resolution depends on the number of collected photons required for good signal-to-noise ratio. Typically, single fluorophores are imaged at rates of 200 Hz or less, with a maximum number of emitted photons before photobleaching near 10^6 :

1. N2a cells expressing 4M5.3-prp chimera are grown in glass-bottom culture dish (Mattek Corp.) for room temperature imaging. Alternatively, cells are imaged using the 6-well glass-bottom chamber plates (Wafergen, CA) that can be programmed for imaging at 37 °C.
2. Switch to bright-field imaging to focus onto a region of interest and record this image. If desired, record a DIC image of the cells.
3. To image FL-QDs, the samples are excited by a fiber-coupled 488-nm laser line at 2–5 mW from an argon laser. Images are further magnified and filtered through a band pass filter (620BP40 Semrock) for FL-QD imaging. In the case of dual-color imaging, FL-QDs and GFPs are imaged simultaneously by a custom-built dual-view system with dichroic mirror 560LP and filters 628BP40 and 525BP50 for the red and green channel, respectively.
4. Using the fluorescence excitation, focus on the cells and record a fluorescence image.
5. Switch to TIRF angle mode and adjust the focus to the basal membrane of individual adherent cells. Individual fluorescent spots can be detected with the camera or through the eye pieces. Acquire a TIRF image if desired.
6. A sequence of images can then be acquired to follow the movement of individual fluorescent spots. In our experiments, a minimum of 1000 frames at 100 ms per frame is typically recorded for single-particle tracking as seen in [Fig. 3.4A and B](#).
7. Single-particle tracking is performed using custom in-house software (AsteriX) written in LabVIEW ([Pinaud *et al.*, 2009](#)). Briefly, individual QD images are fitted by a Gaussian intensity profile, resulting in sub-pixel determination of the center position. Single-particle trajectories can then be analyzed by different approaches, as described ([Pinaud *et al.*, 2009](#)).
8. Fluorescent intensity along a single-time trace (camera photo counts per frame) along the trajectory is the determining factor to exclude aggregate from single FL-pc-QDs. A blinking intensity time trace is characteristic of a single QD, illustrated in [Fig. 3.4C and D](#), but is not a necessary condition. Absolute time trace intensity significantly larger than the average may indicate the observation of an aggregate, especially if no blinking is observed.

ACKNOWLEDGMENTS

We thank Professor Wittrup for providing the 4M5.3 scFv plasmid, Professor Lindquist for the mouse PrP plasmid, and Dr. Thomas Dertinger for help with FACS data import. We acknowledge the help of Dr. Ingrid Schmid, supervisor of the UCLA Jonsson Comprehensive Cancer Center (JCCC) and Center for AIDS Research Flow Cytometry Core Facility that is supported by National Institutes of Health awards CA-16042 and AI-28697, and by the JCCC, the UCLA AIDS Institute, and the David Geffen School of Medicine at UCLA.

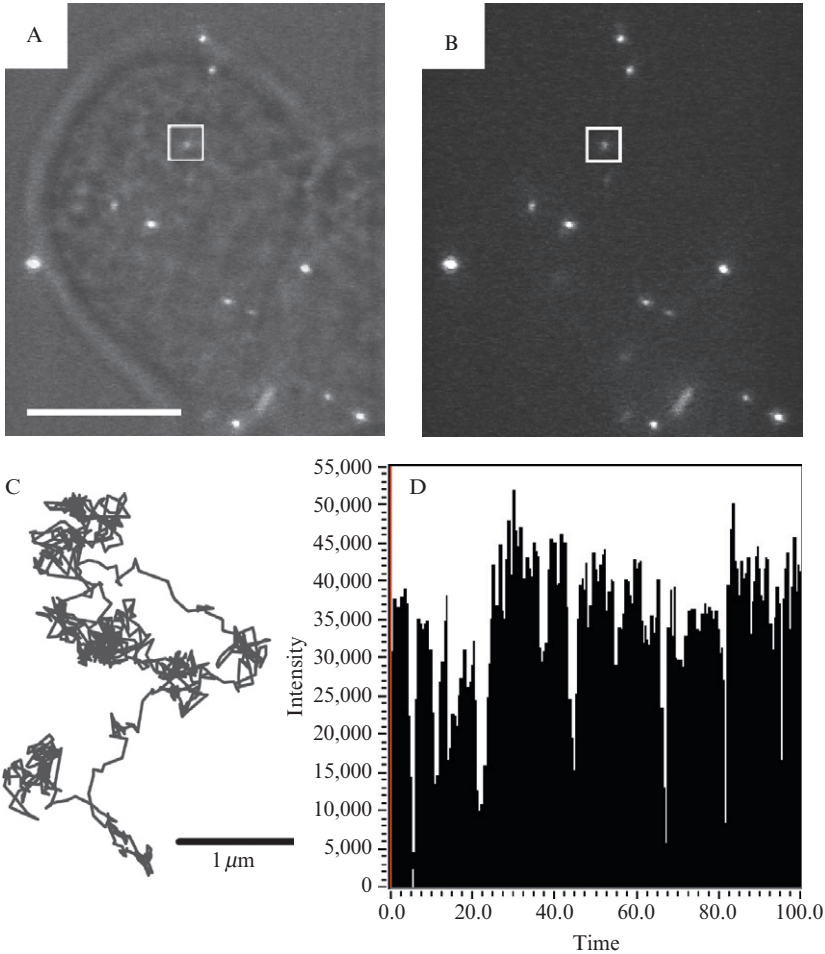


Figure 3.4 Imaging of scFv-PrP with FL-QDs in live N2a cells. (A) DIC image overlaid with QD signal (white dots), scale bar = 10 μm . (B) Fluorescent image. (C) 1000 frames single-QD trajectory of QD indicated in white square. (D) Intensity time trace (camera counts per frame) along the trajectory exhibiting a blinking pattern of single QD. Iyer G, Pinaud F, Tsay J, Weiss S : Solubilization of quantum dots with a recombinant peptide from *Escherichia coli*. Small Vol 3. Issue 5 Pages 793–798. Copyright Wiley-VCH Verlag GmbH & Co. KGaA. Reproduced with permission.

Ensemble confocal imaging was performed at the UCLA/CNSI Advanced Light Microscopy Shared Facility. This work was supported by NIH/NIBIB BRP Grant 5-R01-EB000312 and the NSF, The Center for Biophotonics, an NSF Science and Technology Center managed by the University of California, Davis, under Cooperative Agreement PHY0120999.

REFERENCES

- Andresen, M., Schmitz-Salue, R., and Jakobs, S. (2004). Short tetracysteine tags to β -tubulin demonstrate the significance of small labels for live cell imaging. *Mol. Biol. Cell.* **15**, 5616–5622.
- Betzig, E., Patterson, G. H., Sougrat, R., Lindwasser, O. W., Olenych, S., Bonifacino, J. S., Davidson, M. W., Lippincott-Schwartz, J., and Hess, H. F. (2006). Imaging intracellular fluorescent proteins at nanometer resolution. *Science* **313**, 1642–1645.
- Bhunia, A. K., and Miller, S. C. (2007). Labeling tetracysteine-tagged proteins with a SplAsH of color: A modular approach to bis-arsenical fluorophores. *Chem. Bio. Chem.* **8**, 1642–1645.
- Boder, E. T., and Wittrup, K. D. (2000). Yeast surface display for directed evolution of protein expression, affinity, and stability. *Meth. Enzymol.* **328**, 430–444.
- Boder, E. T., Midelfort, K. S., and Wittrup, K. D. (2000). Directed evolution of antibody fragments with monovalent femtomolar antigen-binding affinity. *Proc. Natl. Acad. Sci. USA* **97**, 10701–10705.
- Brichta, J., Hnilova, M., and Viskovic, T. (2005). Generation of hapten-specific recombinant antibodies: antibody phage display technology: A review. *Vet. Med. Czech.* **50**, 231–252.
- Bruchez, M., Jr., Moronne, M., Gin, P., Weiss, S., and Alivisatos, A. P. (1998). Semiconductor nanocrystals as fluorescent biological labels. *Science* **281**, 2013–2016.
- Carrico, I. S., Carlson, B. L., and Bertozzi, C. R. (2007). Introducing genetically encoded aldehydes into proteins. *Nat. Chem. Biol.* **3**, 321–322.
- Chang, Y. P., Pinaud, F., Antelman, J., and Weiss, S. (2008). Tracking bio-molecules in live cells using quantum dots. *J. Biophoton* **1**, 287–298.
- Chao, G., Lau, W. L., Hackel, B. J., Sazinsky, S. L., Lippow, S. M., and Wittrup, K. D. (2006). Isolating and engineering human antibodies using yeast surface display. *Nat. Protoc.* **1**, 755–768.
- Chudakov, D. M., Lukyanov, S., and Lukyanov, K. A. (2005). Fluorescent proteins as a toolkit for in vivo imaging. *Trends Biotechnol.* **23**, 605–613.
- Dabbousi, R. O., Rodriguez-Viejo, J., Mikulec, F. V., Heine, J. R., Mattoussi, H., Ober, R., Jensen, K. F., and Bawendi, M. G. (1997). (CdSe)ZnS core-shell quantum dots: synthesis and characterization of a size series of highly luminescent nanocrystallites. *J. Phys. Chem. B* **101**, 9463–9475.
- Dahan, M., Levi, S., Luccardini, C., Rostaing, P., Riveau, B., and Triller, A. (2003). Diffusion dynamics of glycine receptors revealed by single-quantum dot tracking. *Science* **302**, 442–445.
- Duckworth, B. P., Zhang, Z., Hosokawa, A., and Distefano, M. D. (2007). Selective labeling of proteins by using protein farnesyltransferase. *Chem. Bio. Chem.* **8**, 98–105.
- George, N., Pick, H., Vogel, H., Johnsson, N., and Johnsson, K. (2004). Specific labeling of cell surface proteins with chemically diverse compounds. *J. Am. Chem. Soc.* **126**, 8896–8897.
- Giepmans, B. N., Adams, S. R., Ellisman, M. H., and Tsien, R. Y. (2006). The fluorescent toolbox for assessing protein location and function. *Science* **312**, 217–224.
- Hibino, K., Hiroshima, M., Takahashi, M., and Sako, Y. (2009). Single-molecule imaging of fluorescent proteins expressed in living cells. *Meth. Mol. Bio.* **544**, 451–460.
- Hoffmann, C., Gaietta, G., Bünemann, M., Adams, S. R., Oberdorff-Maass, S., Behr, B., Vilardaga, J. P., Tsien, R. Y., Ellisman, M. H., and Lohse, M. J. (2005). A FAsH-based FRET approach to determine G protein – Coupled receptor activation in living cells. *Nat. Meth.* **2**, 171–176.
- Howarth, M., and Ting, A. Y. (2008). Imaging proteins in live mammalian cells with biotin ligase and monovalent streptavidin. *Nat. Protocols* **3**, 534–545.

- Howarth, M., Takao, K., Hayashi, Y., and Ting, A. Y. (2005). Targeting quantum dots to surface proteins in living cells with biotin ligase. *Proc. Natl. Acad. Sci. USA* **102**(21), 7583–7588.
- Iyer, G., Pinaud, F., Tsay, J., and Weiss, S. (2007). Solubilization of quantum dots with a recombinant peptide from *Escherichia coli*. *Small* **3**, 793–798.
- Iyer, G., Michalet, X., Chang, Y. P., Pinaud, F. F., Matyas, S. E., Payne, G., and Weiss, S. (2008). High affinity scFv-hapten pair as a tool for quantum dot labeling and tracking of single proteins in live cells. *Nano Letters* **8**, 4618–4623.
- Joo, C., Balci, H., Ishitsuka, Y., Buranachai, C., and Ha, T. (2008). Advances in single-molecule fluorescence methods for molecular biology. *Ann. Rev. Biochem.* **77**, 51–76.
- Kwon, G. S., and Hadjantonakis, A.-K. (2007). Eomes::GFP – A tool for live imaging cells of the trophoblast, primitive streak, and telencephalon in the mouse embryo. *Genesis* **45**, 208–217.
- Lin, C. W., and Ting, A. Y. (2006). Transglutaminase-catalyzed site-specific conjugation of small-molecule probes to proteins in vitro and on the surface of living cells. *J. Am. Chem. Soc.* **128**, 4542–4543.
- Lippincott-Schwartz, J., and Patterson, G. (2003). Development and use of fluorescent protein markers in living cells. *Science* **300**, 87–91.
- Los, G. V., Encell, L. P., McDougall, M. G., Hartzell, D. D., Karassina, N., Zimprich, C., Wood, M. G., Learish, R., Ohana, R. F., Urh, M., Simpson, D., Mendez, J., *et al.* (2008). HaloTag: A novel protein labeling technology for cell imaging and protein analysis. *ACS Chem. Biol.* **3**(6), 373–382.
- Michalet, X., Michalet, X., Kapanidis, A. N., Laurence, T., Pinaud, F., Doose, S., Pflughoeft, M., and Weiss, S. (2003). The power and prospects of fluorescence microscopies and spectroscopies. *Ann. Rev. Biophys. Biomol. Struct.* **32**, 161–182.
- Michalet, X., Pinaud, F. F., Bentolila, L. A., Tsay, J. M., Doose, S., Li, J. J., Sundaresan, G., Wu, A. M., Gambhir, S. S., and Weiss, S. (2005). Quantum dots for live cells, in vivo imaging, and diagnostics. *Science* **307**, 538–544.
- Miller, L. W., Sable, J., Goelet, P., Sheetz, M. P., and Cornish, V. W. (2004). Methotrexate conjugates: A molecular in vivo protein tag. *Angew Chem. Intl. Ed.* **43**, 1672–1675.
- Miller, L. W., Cai, Y., Sheetz, M. P., and Cornish, V. W. (2005). In vivo protein labeling with trimethoprim conjugates: a flexible chemical tag. *Nat. Meth.* **2**, 255–257.
- Murray, C. B., Norris, D. J., and Bawendi, M. G. (1993). Synthesis and characterization of nearly monodisperse CdE (E = S, Se, Te) semiconductor nanocrystallites. *J. Am. Chem. Soc.* **115**, 8706–8715.
- Peng, X., Schlamp, M. C., Kadavanich, A. V., and Alivisatos, A. P. (1997). Epitaxial growth of highly luminescent CdSe/CdS core/shell nanocrystals with photostability and electronic accessibility. *J. Am. Chem. Soc.* **119**, 7019–7029.
- Pinaud, F., King, D., Moore, H.-P., and Weiss, S. (2004). Bioactivation and cell targeting of semiconductor CdSe/ZnS nanocrystals with phytochelatin-related peptides. *J. Am. Chem. Soc.* **126**, 6115–6123.
- Pinaud, F., Michalet, X., Iyer, G., Margeat, E., Moore, H. P., and Weiss, S. (2009). Dynamic partitioning of a glycosyl-phosphatidylinositol-anchored protein in glycosphingolipid-rich microdomains imaged by single-quantum dot tracking. *Traffic* **10**, 691–712.
- Pons, T., and Mattoussi, H. (2009). Investigating biological processes at the single molecule level using luminescent quantum dots. *Ann. Biomed. Eng.* **37**(10), 1934–1959.
- Roullier, V., Clarke, S., You, C., Pinaud, F., Gouzer, G. G., Schaible, D., Marchi-Artzner, V., Piehler, J., and Dahan, M. (2009). High-affinity labeling and tracking of individual histidine-tagged proteins in live cells using Ni²⁺ tris-nitrilotriacetic acid quantum dot conjugates. *Nano Letters* **9**, 1228–1234.
- Sakaue-Sawano, A., Kurokawa, H., Morimura, T., Hanyu, A., Hama, H., Osawa, H., Kashiwagi, S., Fukami, K., Miyata, T., Miyoshi, H., Imamura, T., Ogawa, M., *et al.*

- (2008). Visualizing spatiotemporal dynamics of multicellular cell-cycle progression. *Cell* **132**, 487–498.
- Tsien, R. Y. (1998). The green fluorescent protein. *Annu. Rev. Biochem.* **67**, 509–544.
- Villalobos, V., Naik, S., and Piwnica-Worms, D. (2007). Current state of imaging protein–protein interactions in vivo with genetically encoded reporters. *Annu. Rev. Biomed. Eng.* **9**, 321–349.
- Wacker, S. A., Oswald, F., Wiedenmann, J., and Knöchel, W. (2007). A green to red photoconvertible protein as an analyzing tool for early vertebrate development. *Dev. Dyn.* **236**, 473–480.
- Wang, T., Tomic, S., Gabdoulline, R. R., and Wade, R. C. (2004). How optimal are the binding energetics of barnase and barstar? *Biophys. J.* **87**, 1618–1630.
- Watanabe, T. M., and Higuchi, H. (2007). Stepwise movements in vesicle transport of HER2 by motor proteins in living cells. *Biophys. J.* **92**, 4109–4120.
- Weber, P., Ohlendorf, D. H., Wendoloski, J. J., and Salemme, F. R. (1989). Structural origins of high-affinity biotin binding to streptavidin. *Science* **243**, 85–88.
- Wennmalm, S., and Simon, S. M. (2007). Studying individual events in biology. *Annu. Rev. Biochem.* **76**, 419–446.
- Westphal, V., Rizzoli, S. O., Lauterbach, M. A., Kamin, D., Jahn, R., and Hell, S. W. (2008). Video-rate far-field optical nanoscopy dissects synaptic vesicle movement. *Science* **320**, 246–249.
- Yu, W. W., Qu, L., Guo, W., and Peng, X. (2003). Experimental determination of the extinction coefficient of CdTe, CdSe, and CdS nanocrystals. *Chem. Mater.* **15**, 2854–2860.
- Zhou, M., and Ghosh, I. (2007). Quantum dots and peptides: A bright future together. *Pept. Sci.* **88**, 325–339.